Predicting the future with Pantheon+TRGB data: some derivations, tabulated results, figures

Michael L. Smith, Abdullah Alsakka, Ahmet M. Öztaş

Abstract

Derivations, results, figures and tables, not included in published chapter "Predicting the future with Pantheon+ and TRGB data; better analytical techniques with the Friedmann-Lemaître-Robertson-Walker models" of the IntechOpen book *Cosmology Research - Addressing Current Problems with Astrophysics*. This repository includes tabulated results of analyses using Pantheon+TRGB data (18 emissions) of Freedman et al. 2019.

1. Model Derivations

1.1. Expanding universe

We derive useful solutions using the Friedmann approximations by presuming normalised, unit-less parameters constrained as

$$1 = \Omega_m + \Omega_r + \Omega_\Lambda + \Omega_k. \tag{1}$$

These four parameters are linearly related to the Hubble flow as

$$\left(\frac{\dot{a}}{a}\right)^2 = H_0^2 \left(\frac{\Omega_m}{a^3} + \frac{\Omega_r}{a^4} + \Omega_\Lambda + \frac{\Omega_k}{a^2}\right) \tag{2}$$

with H_0 the Hubble constant, Ω_m for matter, Ω_r for radiation (photons), Ω_Λ from the cosmological constant (dark energy, DE), Ω_k for empty space and a the expansion factor with $\frac{\dot{a}}{a}$ having units of velocity/distance.

The Ω_r term is often discarded as being too small to affect the Hubble flow even though the photon number is very large, reducing Eq. (2) to

$$\left(\frac{\dot{a}}{a}\right)^2 = H_0^2 \left(\frac{\Omega_m}{a^3} + \Omega_\Lambda + \frac{\Omega_k}{a^2}\right). \tag{3}$$

Email addresses: `*correspondence mlsmith55@gmail.com` (Michael L. Smith), `abdullah.alsakka.5356@student.uu.se` (Abdullah Alsakka), `oztas@hacettepe.edu.tr` (Ahmet M. Öztaş)

Multiplying through by a^2 gives us an equation of our current state in an expanding universe

$$\left(\frac{da}{dt}\right)^2 == H_0^2\left(\frac{\Omega_m}{a} + \Omega_\Lambda a^2 + \Omega_k\right). \tag{4}$$

Taking the square root of both sides

$$\frac{da}{dt} = H_0\sqrt{\frac{\Omega_m}{a} + \Omega_\Lambda a^2 + \Omega_k} \tag{5}$$

and inverting, prepares a solution for integration by separating the variables

$$dt = \frac{1}{H_0}\frac{da}{\sqrt{\frac{\Omega_m}{a} + \Omega_\Lambda a^2 + \Omega_k}}. \tag{6}$$

We integrate both sides from any selected moment to the present

$$t_0 - t = \frac{1}{H_0}\int_a^1 \frac{da}{\sqrt{\frac{\Omega_m}{a} + \Omega_\Lambda a^2 + \Omega_k}}. \tag{7}$$

Keep in mind the current expansion factor is 1 and allow the usual c=1 in Eq. (7). One can easily calculate the lookback time if the three parameter values are known and substitute a with $\frac{1}{1+z}$.

1.2. General solution

We derive Eqs. (8) and (10) beginning with Eqs. (7) and (14). These derivations will help the reader understand the inconsistencies present in some current literature. A general version of the FLRW model includes parameters for matter density, Ω_m, the normalised cosmological constant, Ω_Λ and empty space, Ω_k. The FLRW solution for use with D_L and z, where $\xi = 1/(1+z)$ is

$$D_L = \frac{c}{H_0\xi\sqrt{|\Omega_k|}}\left[sin\mathrm{n}\left(\sqrt{|\Omega_k|}\int_{\xi_1}^1 \frac{d\xi_1}{\xi_1\sqrt{\frac{\Omega_m}{\xi_1} + \Omega_\Lambda\xi_1^2 + \Omega_k}}\right)\right]. \tag{8}$$

One version of the Standard model includes Ω_Λ with $\Omega_k = 0$ where the normalisation condition simplifies to

$$1 = \Omega_m + \Omega_\Lambda. \tag{9}$$

Another condition which presumes *sin*n(x)=x and Eq. (8) is reduced to

$$D_L = \frac{c}{H_0\xi}\int_{\xi_1}^1 \frac{d\xi_1}{\xi_1\sqrt{\frac{\Omega_m}{\xi_1} + \Omega_\Lambda\xi_1^2}} \tag{10}$$

and one can see that any influence of space on H_0 has been removed. For use with the *distance mag vs. z* correlation we follow the published derivation as per Riess *et al.* 1998 [1]

$$D_L = \frac{c(1+z)}{H_0} \int_0^{z'} \frac{dz'}{\sqrt{(1+z')^2(1+\Omega_m z') - z'(2+z')\Omega_\Lambda}}. \tag{11}$$

For use with the *distance mag vs. z* data we must transform the right-hand sides of Eq.(11) by applying

$$distance\ mag\ (\mu) = 5\log_{10}(Eq.\ 11) + 25. \tag{12}$$

Note that *distance mag*, being the product of the $\log_{10}$ function, has no metric.

1.2.1. Robertson-Walker geometry

The k of the Robertson-Walker (R-W) line element is often presented as

$$ds^2 = -dt^2 + a^2(t)\left[\frac{dr^2}{(1-kr^2)} + r^2 d\theta^2 + r^2 sin^2\theta d\phi^2\right] \tag{13}$$

where r, θ and ϕ are radial coordinates. We combine the Friedmann-Lemaître model with the Robertson-Walker geometry, Eq. (13) by allowing $a = \frac{R}{R_0}$ with r the spherical radius and k a parameter from the R-W radial geometry introduced above. The variables R and R_0 represent cosmological distances with the metric of length and

$$\frac{dR_0 r}{dt} = \frac{R_0}{R}(1-kr^2)^{1/2} \tag{14}$$

$$R_0\frac{dr}{dt} = \frac{1}{a}(1-kr^2)^{1/2} \tag{15}$$

with rearrangement becomes

$$R_0\frac{dr}{(1-kr^2)^{1/2}} = \frac{dt}{a} \tag{16}$$

where k is usually limited to values between and include -1 to +1 and must display the metric m^{-2}.

1.2.2. Normalised Friedmann relationship

We now introduce the term representing the space portion of the normalised Friedmann constant

$$\Omega_k = -\frac{\mathbf{k}c^2}{R_0^2 H_0^2} \tag{17}$$

where **k** is the constant from the Friedmann relationships and not the F-W equation. This helps us along the path to develop a relationship correlating D_L with recession velocity, continuing with

$$R_0 \frac{dr}{(1+\Omega_k R_0^2 H_0^2 r^2)^{1/2}} = \frac{dt}{a}. \tag{18}$$

Substituting Eq. (6) for dt we derive the complicated relationship

$$R_0 \frac{dr}{(1+\Omega_k R_0^2 H_0^2 r^2)^{1/2}} = \frac{1}{H_0 a} \frac{da}{\sqrt{\frac{\Omega_m}{a} + \Omega_\Lambda a^2 + \Omega_k}}. \tag{19}$$

Integrating both sides we have

$$R_0 \int_0^r \frac{1}{\sqrt{1+\Omega_k R_0^2 H_0^2 r^2}} dr = \frac{1}{H_0} \int_a^1 \frac{da}{a\sqrt{\frac{\Omega_m}{a} + \Omega_\Lambda a^2 + \Omega_k}} \tag{20}$$

then changing the variable on the left side using $y = \sqrt{\Omega_k} R_0 H_0 r$

$$\frac{1}{H_0\sqrt{\Omega_k}} \int_0^{\sqrt{\Omega_k} R_0 H_0 r} \frac{1}{\sqrt{1+y^2}} dy = \frac{1}{H_0} \int_a^1 \frac{da}{a\sqrt{\frac{\Omega_m}{a} + \Omega_\Lambda a^2 + \Omega_k}}. \tag{21}$$

Removing H_0 from both sides, the integral on the left hand side is $\text{arcsinh}(y)$ so the above becomes

$$\text{arcsinh}(\sqrt{\Omega_k} R_0 H_0 r) = \sqrt{\Omega_k} \int_a^1 \frac{1}{a} \frac{da}{\sqrt{\frac{\Omega_m}{a} + \Omega_\Lambda a^2 + \Omega_k}}. \tag{22}$$

We substitute the relationship $D_m = R_0 r$ and apply this in

$$\text{arcsinh}(\sqrt{\Omega_k} H_0 D_m) = \sqrt{\Omega_k} \int_a^1 \frac{1}{a} \frac{da}{\sqrt{\frac{\Omega_m}{a} + \Omega_\Lambda a^2 + \Omega_k}} \tag{23}$$

to arrive at the observable D_L using and the relationship $D_L = D_m/a$. We have derived the useful expression of

$$H_0 D_L = \frac{c}{a\sqrt{|\Omega_k|}} \text{sin}n \left\{ \sqrt{|\Omega_k|} \int_{a_1}^1 \frac{da_1}{a_1\sqrt{\frac{\Omega_m}{a_1} + \Omega_\Lambda a_1^2 + \Omega_k}} \right\}. \tag{24}$$

We substitute a with $\frac{1}{1+z}$ where z is linearly related to the galactic recession velocity (to avoid using a which is often a coefficient) becoming our Eq. (8). Here *sin*n can be either *sinh(x)*, *sin(x)* or *x*. The proper selection of *sin*n is confusing in the explanation following Eq. (2) in Riess et al. [1] and the exposition about Eqs. (17,25) in Carroll et al. [2]. Likewise, the definitions of an "open" and "closed" universe is confusing in the latter article, being the opposite of the more common usages. We follow the convention of Einstein who preferred quasi-Euclidean to mean a particle travelling in spacetime following a nearly Euclidean path - with a trace of elliptical bent.

1.2.3. When $\Omega_k = 0$

Some suggest that $\Omega_k = 0$ describes a universe with Euclidean geometry [1, 3]. To investigate this view we derive the relationship to be used with astronomical data without employing Ω_k from Eq. (19) by demanding that $\Omega_k = 0$ describes Euclidean geometry so

$$H_0 R_0 dr = \frac{1}{a} \frac{da}{\sqrt{\frac{\Omega_m}{a} + \Omega_\Lambda a^2}}. \tag{25}$$

This can be rearranged to the equation below after integration and reintroduction of c for lightspeed in a form which can be evaluated with data as

$$D_m = \frac{c}{H_0} \int_{a_1}^{1} \frac{da_1}{a_1 \sqrt{\frac{\Omega_m}{a_1} + \Omega_\Lambda a_1^2}}. \tag{26}$$

Remembering that $D_L = D_m/a$ we now have a relationship that correlates luminosity distance with the expansion factor, a, as

$$D_L = \frac{c}{H_0 a} \int_{a_1}^{1} \frac{da_1}{a_1 \sqrt{\frac{\Omega_m}{a_1} + \Omega_\Lambda a_1^2}} \tag{27}$$

where $a = \frac{1}{1+z}$ for use with astronomical data. This cannot be integrated analytically so must be treated numerically. This derivation is more thoughtful than the previous suggestion that terms containing Ω_k "disappear" when Euclidean geometry is assumed [2].

1.3. Einstein-de Sitter models

We present three variations of the general model of a universe, Eq. (8) where one parameter is sometimes ≈ 0. We present these under the banner of Einstein-de Sitter models and evaluate with the SNe Ia data.

1.3.1. E-DS universe with $\Omega_m \approx 0$

We begin with Eq. (8) or Eq. (24) to derive the Einstein-de Sitter universe by setting $\Omega_m \approx 0$ in a universe with only a light sprinkling of matter with a significant value for $\Omega_k > 0$ and allowing ξ to substitute for a, as

$$D_L = \frac{c}{H_0} \frac{1}{\xi \sqrt{|\Omega_k|}} \sinh \left\{ \sqrt{|\Omega_k|} \int_{\xi_1}^{1} \frac{d\xi_1}{\xi_1 \sqrt{\Omega_\Lambda \xi_1^2 + \Omega_k}} \right\}. \tag{28}$$

When $\Omega_\Lambda \approx 0$ this demands $\Omega_k = 1$, and the above collapses to become

$$D_L = \frac{c}{H_0 \xi} \sinh(1 - \xi) \tag{29}$$

which we term the E-DS model. The appearance of sinh is consistent with Einstein's preference that a universe with any matter at all must display quasi-Euclidean space geometry. The results from evaluating Eq. (29) and the *distance mag vs. z* correlation are presented in Table 1 and Figs. 2a, 1a.

1.3.2. ΛE-DS with $\Omega_\Lambda > 0$

The above Eq. (28) can be analysed after integration. As an aid for this we use the substitutions

$$\Omega_\Lambda \xi^2 + \Omega_k = \Omega_k y^2 \quad \textit{and} \quad \xi = \sqrt{\frac{\Omega_k}{\Omega_\Lambda}}(y^2 - 1) \tag{30}$$

$$\begin{aligned} D_L &= \frac{c}{H_0}\frac{1}{\xi\sqrt{\Omega_k}}\sinh\left\{\sqrt{\Omega_k}\int_{\sqrt{\frac{\Omega_\Lambda}{\Omega_k}\xi^2+1}}^{\frac{1}{\sqrt{\Omega_k}}}\frac{1}{\sqrt{\Omega_k}}\frac{dy}{y^2-1}\right\} \\ &= B\left\{\operatorname{arctanh}\left(\sqrt{\frac{\Omega_\Lambda}{\Omega_k}\xi^2+1}\right) - \operatorname{arctanh}\left(\frac{1}{\sqrt{\Omega_k}}\right)\right\} \end{aligned} \tag{31}$$

where

$$B = \frac{c}{H_0}\frac{1}{\xi\sqrt{\Omega_k}}\sinh(). \tag{32}$$

We simplify the above by using the identity $\operatorname{arctanh}(a) - \operatorname{arctanh}(b) = \operatorname{arctanh}(1/a) - \operatorname{arctanh}(1/b)$

$$D_L = B\left\{\operatorname{arctanh}\left(\frac{\sqrt{|\Omega_k|}}{\sqrt{\Omega_\Lambda\xi^2+\Omega_k}}\right) - \operatorname{arctanh}\left(\sqrt{|\Omega_k|}\right)\right\}. \tag{33}$$

We designate this the ΛE-DS model with the results from modelling with astronomical data and $\xi = \frac{1}{1+z}$ presented in Table 1, below.

1.3.3. ENDS with $\Omega_k = 0$

Setting $\Omega_k = 0$ must mean that we presume $\Omega_m + \Omega_\Lambda = 1$. Beginning with Eq. (27) and substituting 1/(1+z)=*a* allows the redshift to become the independent variable. We also substitute the Ω_Λ term with 1-Ω_m to simplify analysis as

$$\begin{aligned} D_L &= \frac{c(1+z)}{H_0}\int_0^{z'}\frac{dz'}{\sqrt{\Omega_m(1+z')^3+\Omega_\Lambda}} \\ &= \frac{c(1+z)}{H_0}\int_0^{z'}\frac{dz'}{\sqrt{\Omega_m(1+z')^3+1-\Omega_m}} \\ &= \frac{c(1+z)}{H_0}\int_0^{z'}\frac{dz'}{\sqrt{1+\Omega_m[(1+z')^3-1]}} \end{aligned} \tag{34}$$

and we term equation below the *mag*ENDS model, after transformation of Eq. (34) into *distance mag* from Eq. (35) with results listed in Table 1

$$distancemag(\mu) = 5\log_{10}(Eq.\ 34) + 25. \tag{35}$$

A recent publication claims this derivation models the Pantheon+ data at least as well as the current Standard model of cosmology [4] and our results support this contention. (We employ a slightly corrected version as our 34.) That author proposes a wrinkle to the de Sitter description of space, which incorporates an idea of Newcomb assuming antipodal points in space. This explanation "corrects" the elliptical geometry of spacetime allowing estimation of the normalised matter density, Ω_m, as well as H_0, presuming Euclidean space geometry.

Another version of this model for testing with D_L and ξ data is

$$D_L = \frac{c}{H_0 \xi} \left\{ \int_{\xi_1}^{1} \frac{d\xi_1}{\sqrt{\frac{\Omega_m}{\xi_1^3} - \Omega_m + 1}} \right\} \tag{36}$$

where c, H_0 and $\xi = \frac{1}{1+z}$ are as usual. Here Ω_Λ, the normalised cosmological constant, is implied as the remainder from the normalisation conditions presuming $\Omega_k = 0$, so is replaced with 1-Ω_m. The results from this version (Table 1) suggest the ENDS approximation is a fair model of our Universe.

The integration limits are not the same for Eqs. (34) and (36) and the lower limit of 0 can be misleading since evaluation at exactly $z = 0$ cannot be made when the location of the Milky Way is used with Eqs. (12) and (35). We present evaluations with the Pantheon+Anand data [5] in Table 1 as the ENDS models.

2. Additional results

2.1. Einstein-de Sitter

The plots for two versions of the Einstein-de Sitter model using the Pantheon+Anand data are presented below. Plots of several more models with these data and some using the Pantheon+Freedman data are presented on the following pages.

3. Statistical tests

3.1. The correlation coefficient

We employ the r^2 routine available as a Python 3 module using the preamble `from sklearn.metrics import r2_score` as a correlation check. In general, the larger the r^2 the better the fit. Since most r^2 here are ≈ 0.99 this test is not very discriminatory.

Table 1: Results from analyses of all 1701 SNe Ia of Pantheon+18 TRGB (Freedman et al. 2019 [6]) emission data. Standard‡ model with only Pantheon+ data from Brout et al. 2022. H_0 as km $s^{-1}Mpc^{-1}$.

model	H_0	Ω_m	Ω_Λ	Ω_k	r^2	**F-stat (10^5)**	χ^2_{red}	**BIC**
2PStandard model, sinn$= x$								
D_LStandard‡	75.8±0.3	0.23±0.02	0.77±0.02	-	0.9895	26.5	1.60	14.77
Standard‡	73.0±0.2	0.35±0.01	0.65±0.01	-	0.9974	3.51	0.44	14.37
Einstein-de Sitter models								
D_LE-DS	66.2±0.2	-	-	≈ 1	0.9186	11.0	1.38	7.35
D_LENDS	71.5±0.2	0.47±0.02	0.53±0.02	0	0.9885	27.7	0.70	14.79
$D_L\Lambda$E-DS	72.1±0.3	-	0.13±0.05	0.87±0.05	0.9812	24.4	1.72	14.79
magE-DS	65.2±0.2	-	-	≈ 1	0.9936	3.07	1.43	7.04
magENDS	70.7±0.2	0.49±0.02	0.51±0.02	0	0.9973	3.68	0.72	14.40
magΛE-DS	70.4±0.1	-	1.0±0.002	-	0.9973	3.72	0.71	14.41
$R_h = ct$ model								
$D_L R_h$	70.4±0.1	-	-	-	0.9885	52.3	0.71	7.34
magR_h	69.8±0.1	-	-	-	0.9972	7.16	0.71	6.95
Arctanh models, sinn$= sinh(x)$								
D_L2PAtanh	70.8±0.2	0.05±0.03	-	0.95±0.03	0.9861	27.1	0.69	14.79
D_L3PAtanh	71.0±0.2	0.001±0.03	-	0.999±0.03	0.9830	17.0	0.69	22.24
mag2PAtanh	70.1±0.2	0.08±0.03	-	0.92±0.03	0.9973	3.69	0.70	14.40
mag3PAtanh	71.4±0.2	0.001±0.02	-	0.999±0.02	0.9973	2.55	0.62	21.85
2PStandard model, sinn$= x$								
D_LStandard	71.5±0.2	0.46±0.02	0.54±0.02	-	0.9885	27.7	0.70	14.79
Standard	70.7±0.2	0.49±0.02	0.51±0.02	-	0.9973	3.69	0.72	14.44
3PStandard model, sinn$= x$								
D_L3PStnd	71.2±0.2	0.001±0.15	0.16±0.13	0.84±0.20	0.9903	19.7	0.69	22.24
mag3Stnd	70.4±0.2	0.001±0.16	0.12±0.13	0.88±0.20	0.9973	2.47	0.71	21.85
3PStandard model, sinn$= sin(x)$								
D_L3PStnd	71.5±0.2	0.46±0.67	0.54±.32	0.00±0.74	0.9886	18.5	0.70	22.24
mag3Stnd	70.7±0.2	0.49±0.66	0.51±0.82	0.00±0.11	0.9973	2.46	0.72	21.85
3PStandard model, sinn$= sinh(x)$								
D_L3PStnd	70.9±0.2	0.10±0.07	0.07±0.08	0.824±0.11	0.9876	18.7	0.69	22.22
mag3PStnd	70.1±0.2	0.08±0.07	0.001±0.09	0.92±0.11	0.9973	2.46	0.70	21.85

3.2. *F test or F-statistic*

We employ a more useful correlation which considers weighted errors as

$$F = \frac{\frac{(wSSM - wSSE)}{P}}{\frac{wSSE}{(N-P)}} \tag{37}$$

where wSSM is the weighted sum of the squared errors about the mean and wSSE is the weighted sum of squared observational errors with P the number of free parameters and N the number of data pairs. The F value increase dramatically, with no upper limit, when the calculation errors are small and the correlation good. The F value also increases with increasing data number. This property allows facile discrimination between good and poor data, and between models, even when models employ different parameter numbers [7]. The F-statistic is a good measure of model fitness for analyses of large ensembles.

3.3. *Pearson's chi-squared test*

The χ^2 commonly used to test model compliance considering observational error is usually calculated as

$$\chi^2 = \sum \left(\frac{(\text{Obs} - \text{Calc})^2}{\text{Calc}} \right) \tag{38}$$

Obs is the observed value and Calc the calculated value of the dependent variable [8, 9, 10]. This version is different from the test preferred by some astronomers where the squared sums of the observed and systematic standard deviations, for both independent and dependent variables, are placed in the denominator as

$$\chi^2 = \sum \left(\frac{(\text{Obs} - \text{Calc})^2}{\sigma^2_{(x)} + \sigma^2_{(y)}} \right) \tag{39}$$

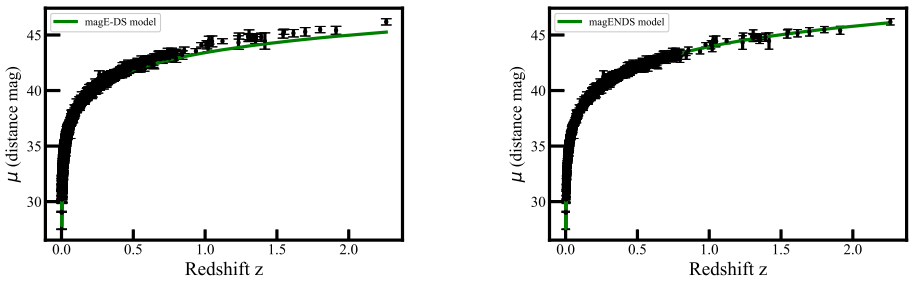

(a) The magE-DS model

(b) The magENDS model

Figure 1: Two Einstein-de Sitter models with Pantheon+TRGB data from Anand, et al. 2022.

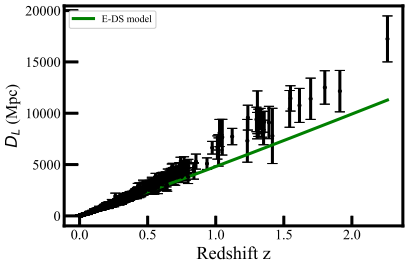

(a) The D_LE-DS model

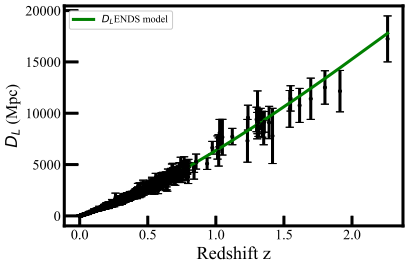

(b) The D_LENDS model

Figure 2: Plots using the Pantheon+TRGB data from Anand et al. (left) or the Pantheon+TRGB data from Freedman et al. (right). Note the distant σ values are larger than nearby events.

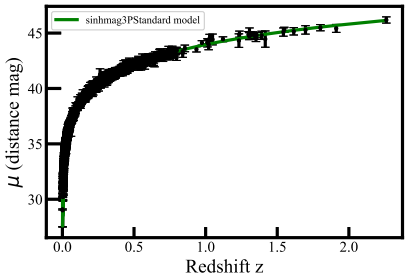

(a) sinh*mag*3PStandard

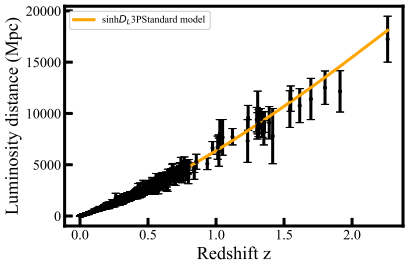

(b) sinhD_L3PStandard

Figure 3: Two versions of the Standard model using 3-parameter regression with Pantheon+TRGB data from Anand et al. 2022.

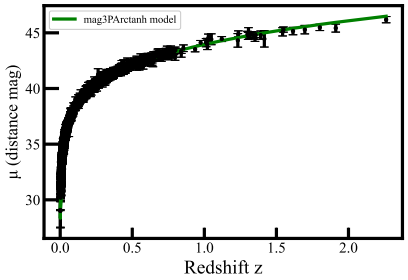

(a) *mag*3PArctanh

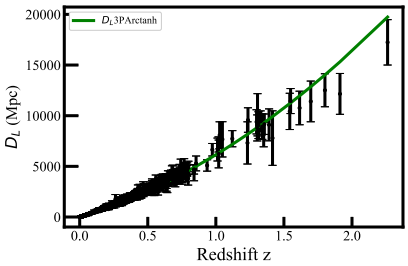

(b) D_L3PArctanh

Figure 4: Two versions of the Standard model using 3-parameter regression with Pantheon+TRGB data from Anand et al. 2022.

according to [1, 11]. Here we ignore $\sigma_{(x)}$ because the errors of redshift measurements are minuscule compared with errors associated with distances [12]. This version of the χ^2 test is problematic when evaluating a system where the origin is known with certainty and $\sigma^2_{(x)} + \sigma^2_{(y)} = 0$. This is the case here as the position and relative velocity of the earth are known exactly. When using Eq. (39) we were forced to introduce a small error to the earth's position ($D_L = 0, \sigma = 0.01$) to solve for χ^2. We use the reduced χ^2 as below for model evaluations

$$\chi^2_{red} = \frac{\chi^2}{N - P} \tag{40}$$

with N and P as above. As a rule, the lower the χ^2_{red} value the better the model. The term χ^2_{red} represents the reduced goodness of fit according to Eq. (39) without considering $\sigma^2_{(x)}$ and we do not report values using Eq. (38).

3.4. Bayesian information criterion

We calculate BIC values using the Python 3 module `from astropy.stats.info_theory` with the routine `bayesian_info_criterion` where the SSE is the sum of the errors squared. There are other similar tests for model worthiness, for example the Akaike information criterion which can be evaluated using some of the subroutines provided. While the BIC statistic is sometimes useful for comparisons across model types with limited data, this test does not seem useful here because the parameter number correction dominates. While BIC supposedly informs us that the E-DS and R_h models are the better than the others, visual inspection of the graphs and the other statistics tell us that the E-DS models are not very good descriptions. The BIC value is really only informative about the number of free parameters which is not news.

4. Correlation types

An irrationality we observed are the compressed $\sigma_{(y)}$ values exhibited by all plots correlating the *distance mag vs. z* data compared with the $\sigma_{(y)}$ values exhibited by the D_L *vs. z* plots. The relative $\sigma_{(y)}$ values are of overriding importance for weighted, computerised evaluations, flawed weighting yields incorrect results. The resulting parameters along with the calculated χ^2_{red} values may be smaller than reality; the usefulness of Ω_m, Ω_Λ and Ω_k calculated using the *distance mag vs. z* correlation is questionable. Another major problem is the unjustified, unaddressed discarding of the data pair with the smallest distance error, the position of our Milky Way. We know exactly where we are and how fast we are moving, relatively. This act introduces systematic error but can be corrected by correlating D_L with z and including the values of 0,0 for our recession velocity and distance.

References

[1] A. G. Riess, et al., Observational Evidence from Supernovae for an Accelerating Universe and a Cosmological Constant, AJ 116 (1998) 1009–1038. doi:10.1086/300499.

[2] S. M. Carroll, et al., The Cosmological Constant, Ann. Rev. A&A 30 (1) (1992) 499–542. doi:10.1146/annurev.aa.30.090192.002435.

[3] B. P. Schmidt, et al., The high-z supernova search: Measuring cosmic deceleration and global curvature of the Universe using type Ia supernovae, ApJ 507 (1) (1998) 46–63. doi:10.1086/306308.

[4] V. N. Yershov, Fitting type Ia supernova data to a cosmological model based on Einstein-Newcomb-de Sitter space, Universe 9 (5) (2023) 204. doi:10.3390/universe9050204.

[5] G. S. Anand, et al., Comparing Tip of the Red Giant Branch Distance Scales: An independent reduction of the Carnegie-Chicago Hubble program and the value of the Hubble constant, ApJ 932 (1) (2022) 15. doi:10.3847/1538-4357/ac68df.

[6] W. L. Freedman, et al., The Carnegie-Chicago Hubble Program. VIII. An independent determination of the Hubble constant based on the Tip of the Red Giant Branch, ApJ 882 (1) (2019) 34. doi:10.3847/1538-4357/ab2f73.

[7] SYSTAT, TableCurve 3D v4 for Windows User's Manual, page D-6, SYSTAT Software Inc., 2002.

[8] S. Khan, R-squared or coefficient of determination (Nov. 2010).
URL `https://www.youtube.com/watch?v=lng4ZgConCM`

[9] J. Fernando, R-squared formula, regression, and interpretations, Investopedia (Sep. 2021).
URL `https://www.investopedia.com/terms/r/r-squared.asp`

[10] A. Hayes, Chi-square statistic, Investopedia (Oct. 2022).
URL `https://www.investopedia.com/terms/c/chi-square-statistic.asp`

[11] A. G. Riess, et al., Type Ia Supernova Discoveries at z>1 from the Hubble Space Telescope: Evidence for Past Deceleration and Constraints on Dark Energy Evolution, ApJ 607 (2) (2004) 665–687. doi:10.1086/383612.

[12] K. Khoshelham, S. O. Elberink, Accuracy and resolution of kinect depth data for indoor mapping applications, Sensors 12 (2) (2012) 1437–1454. doi:10.3390/s120201437.